Kshitij Gaur

Nitish M. Tech final Thesis report

paper-21/05/26

Document Details

Submission ID
trn:oid:::27535:140490587

Submission Date
May 26, 2026, 12:08 PM GMT+5:30

Download Date
May 26, 2026, 12:14 PM GMT+5:30

File Name
Nitish M. Tech final Thesis report.docx

File Size
9.6 MB

50 Pages

9,362 Words

53,277 Characters

8% Overall Similarity

The combined total of all matches, including overlapping sources, for each database.

Match Groups

69 Not Cited or Quoted 7%
Matches with neither in-text citation nor quotation marks

6 Missing Quotations 1%
Matches that are still very similar to source material

1 Missing Citation 0%
Matches that have quotation marks, but no in-text citation

0 Cited and Quoted 0%
Matches with in-text citation present, but no quotation marks

Top Sources

5% Internet sources
4% Publications
5% Submitted works (Student Papers)

Match Groups

- **69** Not Cited or Quoted 7%
  Matches with neither in-text citation nor quotation marks
- **6** Missing Quotations 1%
  Matches that are still very similar to source material
- **1** Missing Citation 0%
  Matches that have quotation marks, but no in-text citation
- **0** Cited and Quoted 0%
  Matches with in-text citation present, but no quotation marks

Top Sources

5% Internet sources
4% Publications
5% Submitted works (Student Papers)

Top Sources

The sources with the highest number of matches within the submission. Overlapping sources will not be displayed.

1	Internet	www.durhamyorkwaste.ca <1%
2	Internet	doczz.net <1%
3	Internet	1library.net <1%
4	Student papers	Anna University on 2026-05-20 <1%
5	Internet	mafiadoc.com <1%
6	Internet	www.mdpi.com <1%
7	Student papers	University of Wolverhampton on 2026-05-23 <1%
8	Internet	www.civil.utm.my <1%
9	Student papers	Higher Education Commission Pakistan on 2019-11-13 <1%
10	Internet	www.iul.ac.in <1%

11 Student papers
Birla Institute of Technology and Science Pilani on 2023-05-30 <1%

12 Publication
Emmanuel Baah-Frempong, Sanjay Kumar Shukla. "Embedded strip footing in a g... <1%

13 Student papers
Teesside University (Blackboard Ultra) on 2026-03-13 <1%

14 Publication
R.H. Jones, J.T. Holden. "Ground Freezing 88 - Proceedings of the Fifth Internation... <1%

15 Internet
macsphere.mcmaster.ca <1%

16 Internet
www.ijrte.org <1%

17 Publication
Meenakshi Singh, Ashutosh Trivedi, Sanjay Kumar Shukla. "Evaluation of geosynt... <1%

18 Student papers
National Institute Of Technology, Tiruchirappalli on 2026-05-21 <1%

19 Internet
data.mitsgwalior.in <1%

20 Internet
download.bibis.ir <1%

21 Student papers
Institute of Graduate Studies, UiTM on 2011-12-12 <1%

22 Publication
Chijioke C. Ikeagwuani. "Comparative Assessment of the Stabilization of Lime-Sta... <1%

23 Publication
Habib Shahnazari, Reza Rezvani, Mohammad Amin Tutunchian. "Post-cyclic volu... <1%

24 Publication
Marić Božica, Lisac Zvonimir, Szavits-Nossan Antun. "Geotechnical Hazards", Tayl... <1%

25 Internet
core.ac.uk <1%

26 Internet
dspace.dtu.ac.in:8080 <1%

27 Internet
www.uotechnology.edu.iq <1%

28 Publication
Araz Hasheminezhad, Halil Ceylan, Sunghwan Kim, Erol Tutumluer. "Evaluation of... <1%

29 Internet
es.scribd.com <1%

30 Internet
mobt3ath.com <1%

31 Internet
www.ejge.com <1%

32 Student papers
Bogazici University on 2025-10-30 <1%

33 Student papers
Central University Of Jharkhand on 2025-05-17 <1%

34 Student papers
The London College UCK on 2025-04-08 <1%

35 Internet
opus.lib.uts.edu.au <1%

36 Internet
tel.archives-ouvertes.fr <1%

37 Internet
tudr.thapar.edu <1%

38 Student papers
University of Derby on 2015-12-16 <1%

39 Internet

ansit-chair <1%

40 Publication

Bashir Ahmed Mir. "Manual of Geotechnical Laboratory Soil Testing", CRC Press, 2... <1%

41 Student papers

Liverpool John Moores University on 2026-05-24 <1%

42 Student papers

North Eastern Regional Institute of Science and Technology on 2021-06-14 <1%

43 Student papers

University of Reading on 2026-05-26 <1%

44 Student papers

Velez College on 2026-05-22 <1%

45 Internet

iugspace.iugaza.edu.ps <1%

46 Internet

keu92.org <1%

47 Internet

open.uct.ac.za <1%

48 Publication

A. Kumar, A.T. Papagiannakis, A. Bhasin, D. Little. "Advances in Materials and Pav... <1%

49 Publication

D.G. Price. "Comptes-rendus sixième congrès international association internatio... <1%

50 Student papers

University of Technology on 2018-04-18 <1%

ABSTRACT

Unpaved roads are largely constructed in rural, mining, and forest areas. They are economic and less labour extensive as compared to paved roads. However, they generally under-perform when subjected to heavy loads and high traffic volume. The major challenges related to unpaved roads are excessive rutting, surface deformation, and reduced serviceability, when built on soft subgrade soils. This leads to higher maintenance cost and compromises overall road safety. A comparative investigation was done using static and dynamic cone penetration test on soft subgrade with and without geosynthetic reinforcement. The geosynthetics compared in this study were geogrid and geotextile. These reinforcements were placed in the soil test section at 50 & 100 mm depths to determine their effects on load distribution & strength improvement. The results of the reinforced sections showed increased cone resistance value, decreased penetration depth, and increased stiffness compared to the unreinforced soil. In static cone penetration test the geogrid reinforced subgrade shows an increase of 225% cone resistance while 144% resistance is achieved using geotextile reinforced at 50 mm and 61.36% cone resistance while 41.09% resistance is achieved using geotextile reinforced at 100 mm when compared to unreinforced section. In dynamic cone penetration test the geogrid reinforced subgrade shows an increase of 300% cone resistance while 200% resistance is achieved using geotextile reinforced at 50 mm and 200% cone resistance while 166.67% resistance is achieved using geotextile reinforced at 100 mm when compared to unreinforced section. These improvements may contribute to durability of the road, lower maintenance costs, and better road safety. The study will help the field practitioners to efficiently place these reinforcements for suitable applications.

LIST OF CONFERENCES / PUBLICATIONS

1. Kumar, N., Gaur, K., and Trivedi, A. (2026). Effect of geosynthetic reinforcement in unpaved road using static cone penetration test. In *5th International Conferences on Advances in Science, Engineering & Technology (ICASET).*
2. Kumar, N., Gaur, K., and Trivedi, A. (2026). Improvement of soft subgrade using geosynthetics: A dynamic cone penetration test investigation. In *International Conferences on Geotechnical Engineering and Civil Engineering Solutions (ICGECE).*
3. Roy, P., Kumar, N., Gaur, K., and Trivedi, A. (2026). Effect of geogrid and bamboo-grid reinforcement in soil subgrade using dynamic cone penetration test. In *International Conferences on Geotechnical Engineering and Civil Engineering Solutions (ICGECE).*

TABLE OF CONTENT

CONTENT

LIST OF TABLES

LIST OF FIGURES

LIST OF SYMBOLS, ABBREVIATIONS AND NOMENCLATURE

G_s: Specific gravity

W_s: Weight of solids

V_s: Volume of solids

Υ_w: Unit weight of water

C_u: Coefficient of uniformity

C_c: Coefficient of curvature

c: Cohesion

ϕ: Angle of internal friction

&: And

μ: Micron

kg: Kilogram

kN: Kilo Newton

Fig.: Figure

mm: Milli meter

IS: Indian standard

cc: cubic centimeter

cm: Centimeter

m: Meter

g: Gram

H: Tank depth

m^2: Square meter

SP: Poorly graded sand

SW: Well graded sand

CBR: California bearing ratio

SCPT: Static cone penetration test

DSCPT: Digital static cone penetration test

MDD: Maximum dry density

LVDT: Linear variable displacement transducer

OMC: Optimum moisture content

DCPI: Dynamic cone penetration index

USB: Universal serial bus

MD: Machine direction

CMD: Cross – machine direction

Lab.: Laboratory

ITS: Intelligent transportation system

DCP: Dynamic cone penetrometer

APT: Accelerated pavement testing

M. Tech: Master of Technology

DTU: Delhi Technological University

DCPT: Dynamic cone penetration test

DST: Direct shear test

CHAPTER 1

INTRODUCTION

Unpaved roads are commonly constructed in rural and low-traffic regions due to their economical and simple construction. When such roads are laid over weak subgrade soils, they are highly susceptible to rutting, surface deformation, and early deterioration. Use of geosynthetic reinforcements has shown considerable potential in enhancing pavement performance. These materials improve load transfer, minimize and contribute to better structural stability and longer performance life. Evaluates comparative reinforcement performance of geotextile & geogrid in unpaved test sections by field & laboratory investigations, with subgrade improvement estimate using the dynamic cone penetrometer (DCP) (Singh et al., 2020). This study experimental investigation and sustainability assessment of ground improvement of expansive soils. To examine how these advanced methods enhance the strength and long-term performance of infrastructure constructed on expansive soils, leading to more durable, economical, and sustainable (Puppala et al., 2025). Geosynthetics such as geotextiles and geogrids are used to improve strength, stability, and drainage in road construction. Traditional geotextiles have limited drainage capacity under unsaturated conditions. To overcome this, a new wicking geosynthetic composite combining geogrid and wicking nonwoven geotextile has been developed. This study evaluates its ability to enhance drainage, stiffness, and bearing capacity of weak subgrades through model tests (Liu et al., 2025). This study investigations variations in reinforcement section, degrees of compaction, and specimen sizes influence the performance characteristics of silt when reinforced with wicking geotextiles (Guo et al., 2025). Evaluating the effect of geosynthetic as a reinforcement placement depth and layering using the DSCPT to determine most effective configuration for improving subgrade performance. In modern pavement engineering, ensuring long-term stability and durability of road foundations is essential for sustainable infrastructure. Weak subgrade soils often lead to premature road failures, making soil reinforcement techniques an important solution (Boban et al., 2024). This research examines the performance of subgrade soil reinforced with geosynthetic in low-traffic pavements through field testing. It estimates the structural response and overall performance of the reinforced sections and compares results with those of conventional unreinforced pavements (Visvanathan et al., 2022). Geogrids are used in pavements to improve the strength and stability of weak subgrades. They help distribute loads evenly, reducing rutting and surface deformation (Tang et al., 2008). Using geotextiles between layers helps prevent this problem by improving

separation and filtration. This study aims to evaluate how effectively geotextiles can control the movement of subgrade fines under repeated traffic loading using accelerated pavement testing (Kermani et al., 2018).

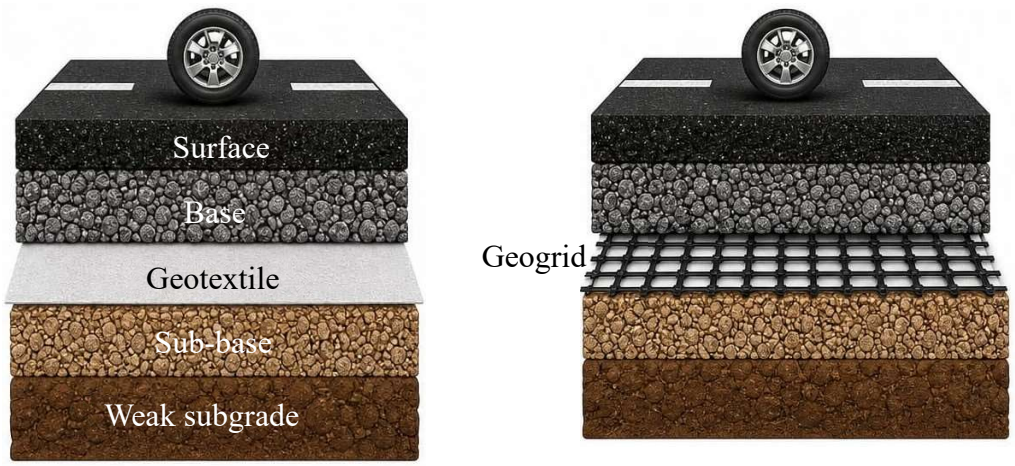

Fig. 1.1 3D schematic illustration of flexible pavement system with (a) Geotextile reinforced (b) Geogrid reinforced

APT as a valuable method to study real-time behavior of such reinforced systems under repeated loads. This research examines the role of geotextile and geocell reinforcement in enhancing subgrade performance under APT conditions. The study aims to contribute toward the design of long lasting and economical pavement structures (Yang et al., 2012). Geosynthetic materials significantly enhance strength & behavior of unpaved roads constructed on weak subgrades. By reinforcing interface between bottom layer & soil subgrade, geosynthetic materials like geotextiles & geogrids help reduce deformation and enhance overall stability (Singh et al., 2020). Expansive soils tend to swell when they absorb water, often causing damage to structures built on them. This problem, researchers have explored reinforcing these soils with discrete synthetic fibers, which help reduce swelling by improving soil–fiber interaction. This study examines how adding polypropylene fibers affects the swelling behavior of expansive soil through laboratory testing (Viswanadham et al., 2009). In this study researchers use geosynthetics material as reinforcement improve soil strength and pavement performance (Singh et al., 2019). This study explores how adding geotextile reinforcement to granular fill can help reduce rutting and improve performance of pavements constructed on soft clay subgrades (Ansari et al., 2021). This study explores a simple and sustainable way to improve road strength by using mine overburden

materials reinforced with coir geotextiles (Rashidian et al., 2018). This study explores how geotextile reinforcement can improve the strength and performance of unpaved roads under repeated loading conditions (Ingle and Bhosale, 2017). This study evaluates how placing geotextile layers within flexible pavement can significantly reduce rutting and improve overall road performance under repeated traffic loads (Sa'adi et al., 2013). Based on detailed review of existing literature it is observable that geosynthetic reinforcement has proven to be an efficient technique for improving strength and stability of weak subgrades. Researchers have reported improvements in CBR, penetration resistance, decrease in rutting and bearing capacity using geotextiles, geogrids, geocells, and natural fiber reinforcements. However, most of the available research is limited to laboratory-scale testing, small model studies, or short-term observations. Only a few studies have employed accelerated pavement testing or dynamic penetration methods to simulate field loading conditions. Moreover, the influence of reinforcement location, number of layers, and reinforcement mechanism under repeated or accelerated loading has not been fully explored. Therefore, there exists a clear research gap in evaluating the performance of geotextile-reinforced subgrades using accelerated or dynamic testing techniques. The present study aims to address these gaps by experimentally investigating the reinforcement effect of geotextile and geogrid on soft subgrade soil using static and dynamic cone penetration test, thereby contributing to practical and performance-based pavement design approaches for unpaved roads and also check soil strength and placement depth of reinforcement like geotextile and geogrid shown in above Figure 1.1.

CHAPTER 2

LITERATURE REVIEW

Conducted a systematic experimental analysis performed to evaluate the effectiveness of reinforcement like geogrid or geotextile or both in unpaved road. Field-scale test sections, including unreinforced, geotextile reinforced, and geogrid reinforced configurations were constructed & tested using DCP and direct shear test. The results clearly demonstrated that the use of geosynthetic reinforcement considerably reduced DCPI values 6.29 mm/blow to 1.91 mm/blow indicating an improvement in subgrade strength. Among the reinforcements studied, geotextile performed better than geogrid, even though geogrid possessed higher tensile strength and stiffness. This behavior was attributed to the better confinement and soil reinforcement interaction provided by geotextiles. Direct shear test result further confirmed enhancement in shear strength of reinforced soils when comparison with unreinforced condition (Singh et al., 2020). Evaluated the individual and combined effects of geosynthetic reinforcement to find strength of silty sand. The experimental result presented both California bearing ratio and UCS value increased significantly with reinforcement with highest improvement observed during geotextile and geogrid were used together. Microstructural analysis using SEM confirmed effective bonding and interlocking between soil particles and reinforcement materials, leading to improved load transfer. The study concluded that combined reinforcement is more effective than single reinforcement in improving weak silty subgrades (Mittal and Shukla, 2018). Compared with geotextile reinforcement and cement stabilization in enhancing load-carrying capacity of sabkha subgrade soils. The findings of the study indicated that geotextiles significantly enhanced subgrade performance under soaked conditions, while cement stabilization achieved higher resilient modulus values, especially at higher cement contents. An economic comparison revealed that geotextile reinforcement provided a better performance to cost-ratio than cement treatment, cement treatment resulted in higher resilient modulus, especially at 10% dosage. The study also developed a mechanistic prediction model to estimate improvements in resilient modulus (Aiban et al., 2006). Experimentally investigated the effect of single and double-layer geosynthetic reinforcement of subgrades. The study observed substantial improvement in California bearing ratio (CBR) values, with double-layer reinforcement showing significantly higher gains compared to single-layer applications. Different geosynthetics exhibited varying optimal placement depths, highlighting that reinforcement efficiency strongly depends on both material type and depth of installation. The

results shows that appropriate selection of reinforcement configuration can greatly enhance load-bearing capacity and durability of unpaved roads (Singh et al., 2019). Conducted full-scale APT to assess the performance of geocell over weak subgrades. The study found that geocell reinforcement significantly reduced rutting and allowed for substantial decreases in base course. Among the materials tested, recycled asphalt pavement (RAP) exhibited the best performance when used as geocell infill (Pokharel et al., 2011). The study demonstrated that geosynthetics significantly reduced rutting and improve pavement service life with double-layer reinforcement providing the best performance. The findings indicated that geosynthetic placed at the subgrade surface primarily stabilized, while additional layers within the base improved load distribution. Despite certain experimental limitations, the research offers strong evidence for incorporating geosynthetics into mechanistic-empirical pavement design practices (Abu-Farsakh et al., 2016). Conducted an extensive evaluation of geogrid properties influencing pavement performance using index testing, bench-scale tests, and accelerated pavement testing. The study concluded that junction strength, tensile stiffness at small strains, aperture size, and flexural rigidity are more critical to pavement performance than ultimate tensile strength. Accelerated pavement testing results showed that stiffer geogrids provided superior rutting resistance, especially over very weak subgrades (Tang et al., 2008). Conducted APT to determine the rutting performance of soft subgrade constructed with geocell reinforcement. The findings showed that geosynthetic reinforcement significantly decreased rutting depth compared to without reinforcement sections under identical loading conditions. The reinforced sand base performed comparably to conventional aggregate bases of similar thickness, demonstrating the effectiveness of geocell confinement. Strain measurements confirmed active load transfer and confinement within the geocell structure, while damaged or broken cells led to reduced performance (Yang et al., 2012). Investigated full-scale accelerated laboratory testing to determine the behavior of geotextile unpaved roads under repeated axle loading. The study reported significant reductions in vertical stress and subgrade deformation, along with improved stress distribution and increased effective CBR. The results demonstrated that geotextile reinforcement enables considerable reduction in base course thickness while maintaining structural performance (Ingle and Bhosale, 2017). Studied the effectiveness of natural jute fiber and synthetic geotextile, both individually and in combination, for improving granular subgrade soil. The findings showed that the combined use of a single geotextile layer with a small percentage of jute fiber produced strength improvements comparable to multiple geotextile layers. Significant increases in soaked and unsoaked CBR values were reported, demonstrating the efficiency of hybrid reinforcement systems (Hossain et al., 2015). Investigated a laboratory-scale to evaluate performance of pavements reinforced with

geogrids, geotextiles, and their combination under static and cyclic loading. The findings indicate all geosynthetic reinforcements improved bearing capacity and reduced settlement; however, the combined geogrid–geotextile system showed the highest performance improvement. Bearing capacity ratio and settlement reduction factor values confirmed that combined reinforcement significantly enhanced pavement life under dynamic loading (Kiptoo et al., 2017).

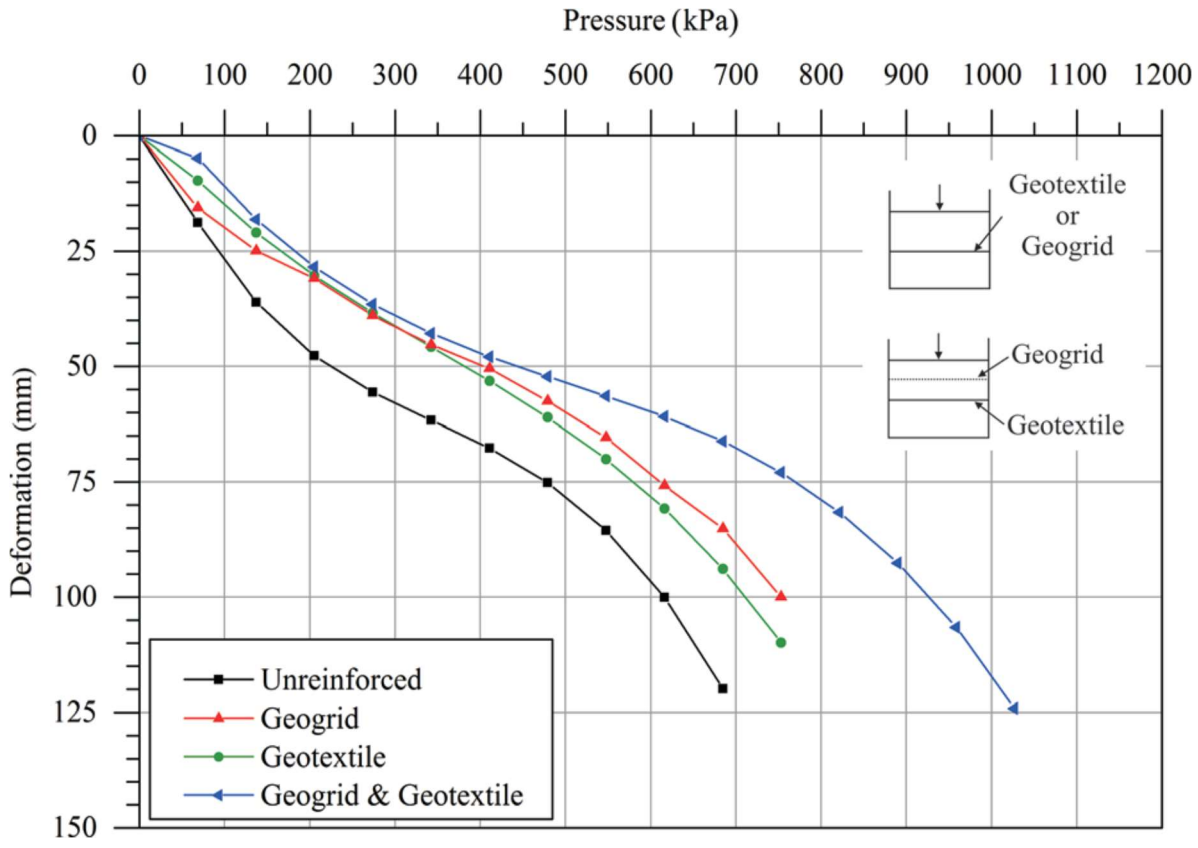

Fig. 2.1 Pressure versus deformation curve (Kiptoo et al., 2017)

The study demonstrated a substantial increase in CBR values when geotextiles were incorporated, particularly when placed at one-fourth depth from the base layer. The results showed that proper placement of geotextile significantly improves reinforcement efficiency, leading to reduced pavement thickness and construction cost (Ogundare et al., 2018). Examined the influence of non-woven geotextile and biaxial geogrid on strength and compaction behavior of weak clayey subgrade soil. The study reported significant improvements in CBR, UCS, and maximum dry density with reinforcement, particularly in triple-layer configurations. SEM analysis confirmed strong interlocking and bonding between soil particles and geosynthetics, leading to improved ductility and load resistance. Despite being limited to laboratory testing, the study clearly demonstrated influence of multi-layer geosynthetics reinforcement in upgrading

subgrade performance and decreasing pavement thickness (Mittal and Shukla, 2019). Conducted a full-scale field investigation to assess the influence of coir geotextile as a sustainable reinforcement for rural road subgrades. The study demonstrated placement of coir geotextile significantly enhanced elastic modulus of subgrade, with enhanced up to 112%, while also allowing reduction of subbase layer thickness. Among the two types tested, the finer coir geotextile (740 g/m²) showed superior performance compared to the coarser variant (365 g/m²), particularly in terms of CBR improvement and long-term pavement stability (Visvanathan et al., 2020). The study demonstrated a significant reduction in penetration resistance values and an increase in CBR for reinforced sections, with geotextile-reinforced pavements outperforming geogrid-reinforced ones. Field results showed considerably higher strength improvement than laboratory findings, emphasizing the importance of in-situ evaluation (Singh et al., 2020). Examined the durability and degradation characteristics of coir geotextiles embedded in various subgrade soils. The study showed that tensile strength loss of coir geotextiles is strongly influenced by soil chemistry, particularly pH, nutrient content, and calcium concentration. Soils with low nutrient content and higher compressibility exhibited lower degradation rates, while acidic and nutrient-rich soils accelerated fiber decay (Sayida et al., 2020). The research indicated that fly ash effectively reduced soil plasticity and enhanced workability, while the inclusion of coir geotextile further improved strength and durability. The combined stabilization method showed a significant higher CBR values compare to untreated soil (Karthik and Chamberlain, 2021). Investigated combined effect of geosynthetic reinforcement on highly plastic subgrade soil. The experimental result illustrated significant increase in both shear strength and unconfined compressive strength, with optimum performance achieved using 0.5% polypropylene fiber in combination with triaxial geogrid. The enhancement in strength was attributed to effective interlocking and stress transfer mechanisms between soil particles, fibers, and geogrids (Tiwari and Satyam, 2022). Investigated the effect of geotextile reinforced on flexible pavements using full-scale field test. The study showed substantial reductions in rut depth, particularly with multi-layer reinforcement systems. Even single-layer reinforcement provided significant performance improvement at relatively low additional cost. The cost–benefit analysis confirmed that modest increases in construction cost resulted in large gains in pavement service life (Al-Saadi et al., 2013). Investigated the feasibility and degradation behavior of jute geotextiles used in road construction over weak subgrades. The study showed that jute geotextiles provide effective separation and filtration during the early life of pavements, despite experiencing rapid strength loss under organic-rich and moist conditions. Denser jute fabrics exhibited better durability compared to lighter variants (Ansari et al., 2021). Evaluated

the shear interaction between subbase & subgrade layers reinforced with different geosynthetics using large scale direct shear test. The result showed biaxial geogrids provided highest interface shear strength for both clay and sand subgrades, while geotextiles exhibited lower performance due to their relatively smooth surfaces. The interaction coefficients highlighted that particle interlocking plays a critical role in shear resistance (Banyhussan et al., 2023). Conducted full-scale APT to determine the reinforcing mechanism of geogrid in pavement systems. The study revealed that geogrid placement within the top one-third of the aggregate layer significantly enhanced rutting resistance, whereas placement at lower depths resulted in inferior performance. Numerical simulations supported the experimental findings by demonstrating improved aggregate confinement and stiffness when tensile strains were mobilized near the surface (Jiang et al., 2024). Experimentally investigated the mechanical strength and deformation characteristics of silt reinforced with wicking geotextiles under varying compaction levels and reinforcement configurations. The results showed that wicking geotextiles substantially improved the strength, ductility, and post-peak stability of silt, particularly at compaction levels of 93–95%. The study revealed that the use of three uniformly spaced reinforcement layers provided the highest strength improvement, with peak strength increases exceeding 200%. In addition, the wicking function enhanced drainage and reduced void ratio, although a slight reduction in compression modulus was observed due to faster consolidation (Guo et al., 2025). Focused on the stabilization of expansive soils using sustainable and eco-friendly materials, including geopolymer treatments, silica fines, and geosynthetics. Laboratory investigations such as unconfined compressive strength, free swell, shrinkage, resilient modulus, and microstructural analysis were carried out. The study revealed that a 30% geopolymer treatment significantly improved strength characteristics while reducing swell–shrink behavior in sulfate-rich expansive soils. The geopolymer-treated soils also showed better resistance to ettringite formation compared to conventional lime stabilization (Puppala et al., 2025).

2.1 Research gaps

A detailed review of the existing literature the following important research gaps:

a. Most previous studies have evaluated either geotextile or geogrid reinforcement individually, while direct comparative studies under identical soil and loading conditions are limited, especially for unpaved road applications.

b. Many investigations are laboratory-scale or model-based, and there is a lack of field-oriented or penetration-based testing methods such as static or dynamic cone penetration tests to assess reinforcement performance realistically.

c. Most investigations have been confined to laboratory-scale strength tests such as CBR, UCS, and plate load tests, whereas penetration-based evaluation methods, such as static or dynamic cone penetration tests, have not been sufficiently explored for reinforced subgrades.

d. The influence of number of reinforcement layers and depth of placement on penetration resistance and subgrade improvement has not been consistently addressed, resulting in no clear consensus on optimal reinforcement configuration.

2.2 Objective of study

The research objectives of the present study are:

a. To investigate the contribution of geosynthetic materials toward strengthening soft subgrade layers in unpaved roads.
b. To evaluate and behavior of reinforced and unreinforced subgrade systems using SCPT and DCPT results.
c. To investigate the impact of varying reinforcement layers on the penetration resistance of weak subgrade.
d. To identify most effective type of reinforcement, namely geotextile or geogrid, in improving subgrade performance under identical test conditions.
e. To identify the most effective reinforcement type and placement depth for improving weak subgrade.

CHAPTER 3

MATERIAL AND METHODOLOGY

3.1 Materials and Methods

The present study utilized sandy soil, geogrid & geotextile as primary materials. Several tests were performed on the sandy soil to evaluate its fundamental properties. The grain size analysis test was carried out to determine the gradation properties of the sandy soil and classify it as SP or SW. The specific gravity of the soil was determined using the pycnometer bottle test. Soil was subjected to a standard proctor test to determine its compaction characteristics including MDD and OMC. The shear strength characteristics of the sandy soil were evaluated using the DST (direct shear test). Soil strength was evaluated using a DSCPT under reinforced and unreinforced conditions. Then DCP test was conducted in the laboratory to evaluate strength of soil. Identify weak zones at different depths, and determine whether the subgrade is suitable for pavement design.

3.2 Sieve Analysis

According to IS:2720 (part 4) – 1985, sieve analysis test was conducted in Soil Mechanics laboratory at DTU to find the gradation characteristics of soil. For sieve analysis test a 1 kg soil sample was taken (shown in Figure 3.1) and passed through 4.75 mm to 75 μ sieve as shown in Figure 3.2. Mass of soil retained on each sieve was measured and the percent finer was calculated. Based on these values particle size distribution curve was presented in Figure 3.3. From grain size distribution curve, the values of D_{10}, D_{30}, & D_{60} were determined as .29, .36 & .45 mm, respectively. Using these parameters C_u and C_c were calculated as 1.55 and 0.99, respectively. Based on the obtained results, soil was classified as SP. The equation used for determining C_u and C_c was following equations 3.1 and 3.2, respectively (Ranjan and Rao, 2011).

$$C_u = \frac{D_{60}}{D_{10}} \quad \text{..... (3.1)}$$

Where C_u = Coefficient of uniformity

D_{60} = Particle diameter corresponding to 60% finer by weight in mm

D_{10} = Effective particle size in mm

$$C_c = \frac{(D_{30})^2}{D_{60} * D_{10}} \quad \text{..... (3.2}$$

Where C_c = Coefficient of curvature

12 D_{30} = Particle diameter corresponding to 30% finer by weight in mm

Table 3.1 Observation and data collection of soil sample using sieve analysis

IS sieve (mm)	Particle size (mm)	Mass retained (g)	Percentage mass retained	Cumulative percentage mass retained	% Finer
4.75	4.75	0	0	0	100
2.00	2.00	4	0.4	0.4	99.60
1.18	1.18	6	0.6	1.0	99.00
0.600	0.600	6	0.6	1.6	98.40
0.300	0.300	862	86.2	87.8	12.20
0.150	0.150	100	10	97.8	2.20
0.075	0.075	20	2	99.8	0.20
Pan	Pan	2	0.2	100	00
		Total = 1000			

Fig. 3.1 Sandy soil (ITS and Soil Dynamics laboratory, DTU, Delhi)

(a)

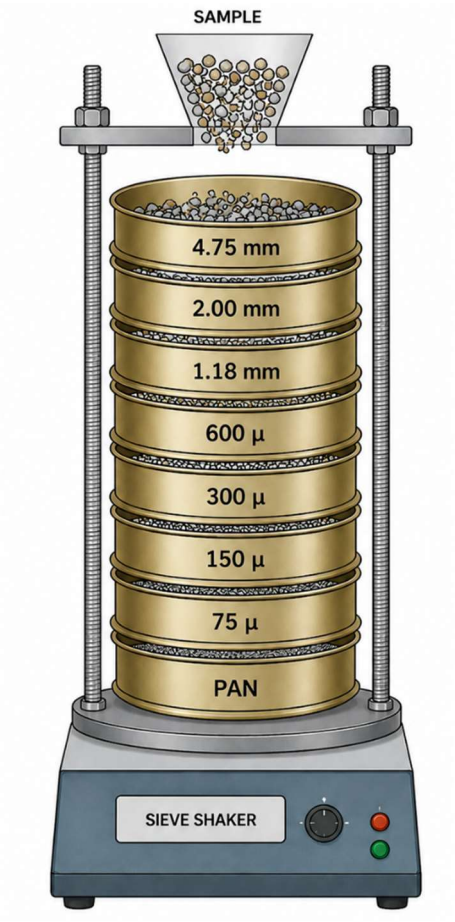

(b)

Fig. 3.2 (a) Sieve analysis experimental setup (Soil Mechanics laboratory, DTU, Delhi) (b) Schematic diagram of sieve analysis setup

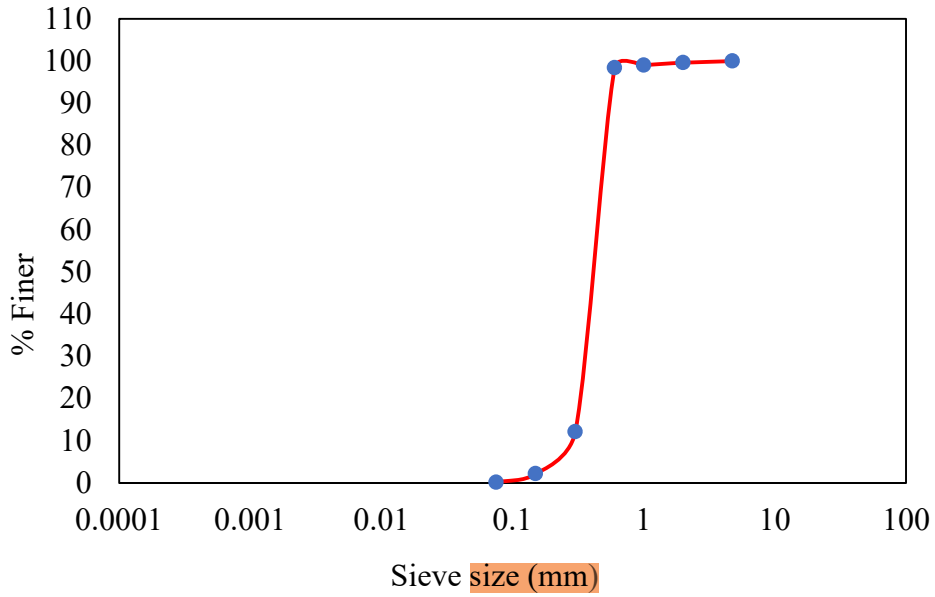

Fig. 3.3 Particle size distribution curve

3.3 Pycnometer Test

As per IS code IS:2720 (part 3) – 1980 pycnometer bottle method was conducted. A sandy soil is taken & passes through 4.75 mm sieve before using. The specific gravity of soil is mainly influenced by density of minerals present in soil particles It represents the ratio between the weight of soil solids and the weight of the same volume of water maintained at 4°C (Ranjan and Rao, 2011). The determined specific gravity of the tested soil sample was found to be 2.66.

$$G_s = \frac{W_s}{V_s \Upsilon_w} \quad \text{..... (3.3)}$$

$$G_s = \frac{\Upsilon_s}{\Upsilon_w} \quad \text{..... (3.4)}$$

Υ_s = Unit weight of solids

$$G_s = \frac{w_2 - w_1}{(w_2 - w_1) - (w_3 - w_4)} \quad \text{..... (3.5)}$$

Where w_1 = Mass of clean empty pycnometer bottle

w_2 = Mass of pycnometer bottle with oven dried soil

w_3 = Mass of pycnometer bottle with soil and water

w_4 = Mass of pycnometer bottle with water

Fig. 3.4 Pycnometer bottle (Soil Mechanics laboratory, DTU, Delhi)

Table 3.2 Observations and calculations specific gravity of soil

Particulars	Test No. 1
w_1 , in g	698
w_2 , in g	1160
w_3 , in g	1868
w_4 , in g	1580
$G_s = \frac{w_2 - w_1}{(w_2 - w_1) - (w_3 - w_4)}$	2.66

3.4 Determination of OMC and MDD

Standard proctor method was conducted in Soil Mechanics laboratory DTU accordance with IS:2720 (part 7) – 1980. According to IS code an oven dried soil sample weighing 3 kg was utilized to conduct standard proctor test. Shown in Figure 3.5 schematic representation of standard proctor apparatus.

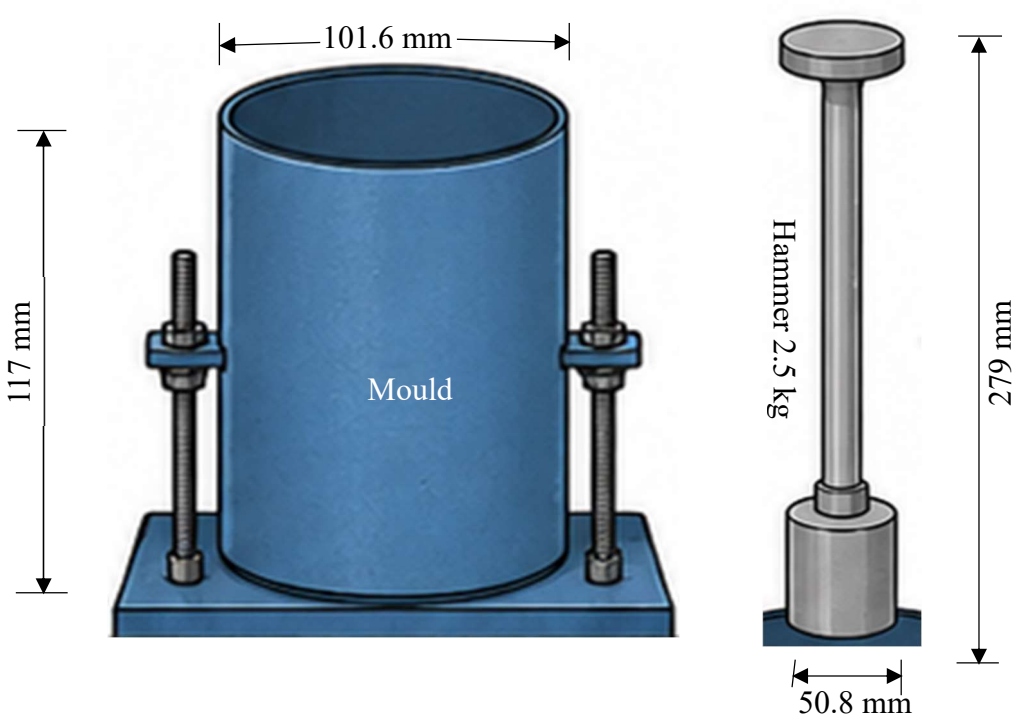

Fig. 3.5 Schematic representation of standard proctor test apparatus

Soil sample was thoroughly added to varying amounts of water from 2% to 10% to obtain different moisture contents.

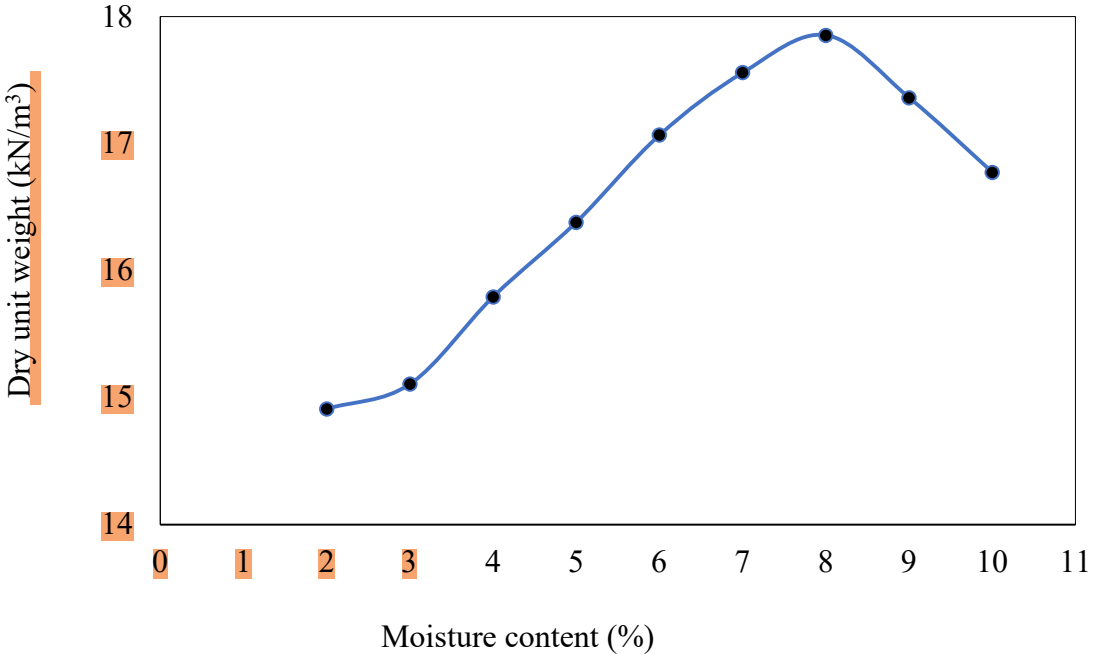

Fig. 3.6 Variation of dry unit weight with moisture content

The soil specimen was filled into the mould in three uniform layers. Each layer was then compacted with 25 hammer blows using a 2.6 kg rammer allowed to fall freely from a height of 310 mm. Weight of soil compacted in mould was determined. The purpose of this test was to evaluate the maximum dry density (MDD) and optimum moisture content (OMC) of the sandy soil. The experiment was carried out repeatedly by varying the moisture content of the soil sample, which are determined from Figure 3.6 as MDD and OMC are 17.854 kN/m^3 and 8%, respectively.

3.5 Direct Shear Test (DST)

Direct shear test was performed in accordance with IS: 2720 (Part 13) – 1986. The sandy soil was placed and compacted inside the shear box (size 60mm x 60mm), which contains a porous stone at the bottom along with the base plate, grid plate, and other supporting components. After placing the grid plates at the top shear box was mounted on the loading frame. A normal load 0.5 kg/cm^2 was first applied on the specimen. Horizontal shear was then applied until the sample failed. During the testing process, the applied shear force and horizontal deformation were measured to determine the cohesion and internal friction angle of the soil. The test was further conducted under higher normal stresses 1.0 & 1.5 kg/cm^2. Direct shear test apparatus is illustrated in Figure 3.7.

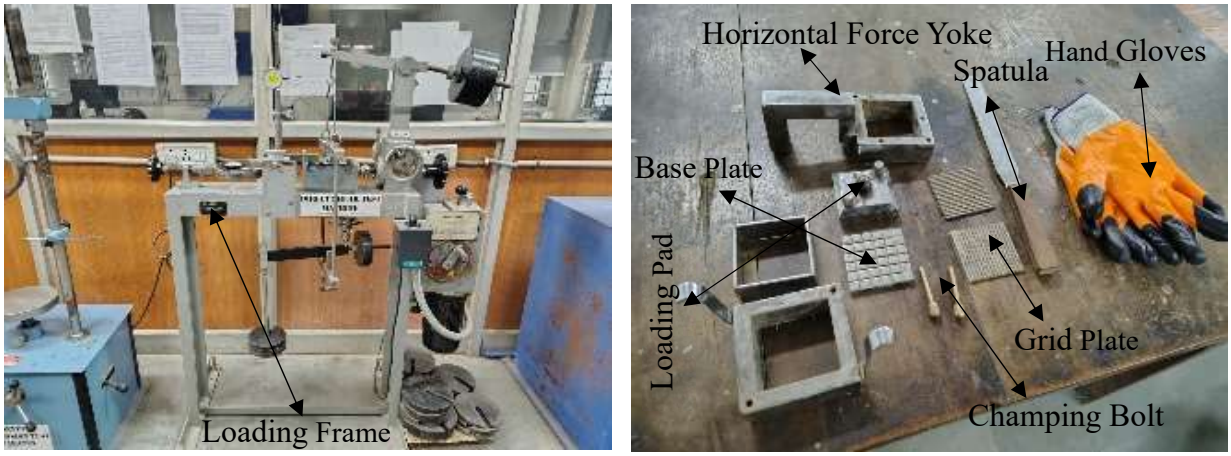

Fig. 3.7 Direct shear test apparatus (Soil Mechanics laboratory, DTU, Delhi)

Table 3.3 Observation and data collection of soil sample using direct shear test

S.I No.	Normal stress (kg/cm^2)	Normal stress (kPa)	Max. Shear stress (kPa)
1	0.5	49.033	5.60
2	1.0	98.067	8.80
3	1.5	147.10	11.96

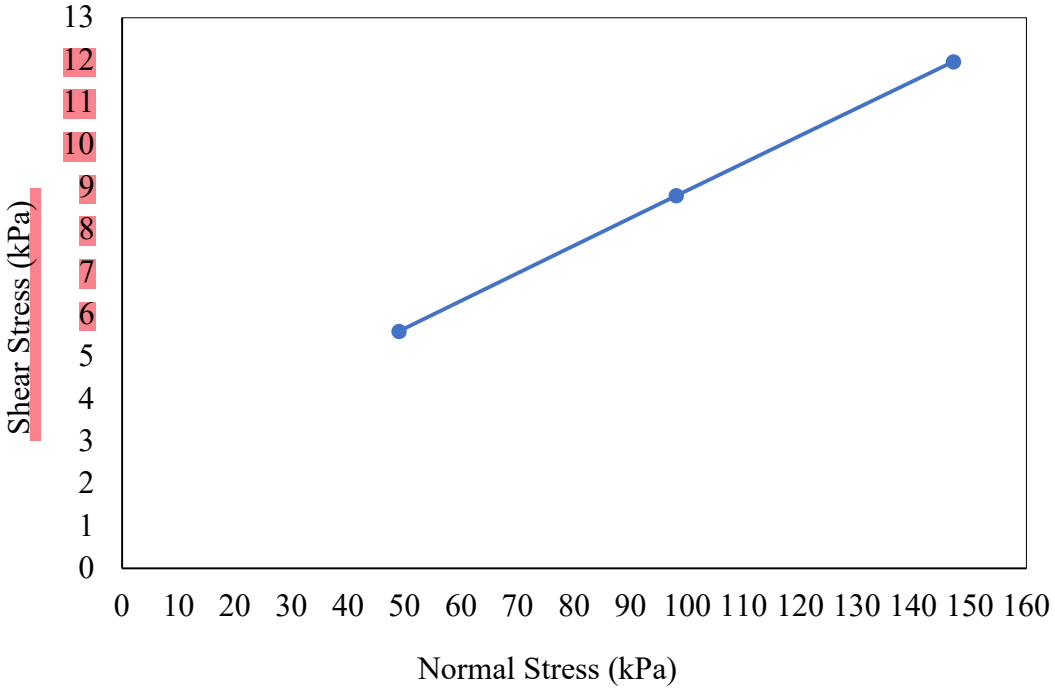

Fig. 3.8 Normal stress v/s shear stress curve

In present study the DST was performed on the soil sample under different normal stresses of 0.5, 1.0, & 1.5 kg/cm². The sample was sheared until failure occurred or a horizontal displacement of 20% was reached in accordance with IS: 2720 (Part 13) – 1986. Based on the recorded shear load and displacement values, a plot between shear stress & normal stress was developed to find the shear strength parameters. From the graph presented in Figure 3.8 cohesion and angle of internal friction were observed as 2.6 kN/m² and 26°, respectively. Fundamental properties of soil used in experimental investigation were presented in Table 3.4.

Table 3.4 Fundamental properties of soil

Characteristics	Results
Material used	Sandy Soil
Grade of soil	Poorly graded sand (SP)
Specific gravity of soil (G_s)	2.66
MDD	17.854 kN/m^3
OMC	8 %
Cohesion (c)	2.6 kN/m^2
Angle of internal friction (ϕ)	26°

3.6 Static Cone Penetration Test

Strength of weak soil surface was evaluated using SCPT in accordance with IS: 4968 (Part 3) – 1976 (Reaffirmed 1987). During the test a hydraulic loading jack was applied to gradually push cone into the ground while cone tip resistance and sleeve friction were measured. In DSCPT apparatus used for this study, two manual push handles are provided to insert the cone into the soil. As shown in Figure 3.9 (Singh et al., 2020), for testing the soil sample was placed inside a steel tank. The experimental setup comprised a load cell, a LVDT, a drive rod measuring 16 mm in Dia and 498 mm in length, and 60° cone fixed at bottom of rod. All readings are recorded through a data acquisition system connected to the load cell and LVDT via a USB output device. The operator applies a steady force using body weight, which pushes the cone downward. The linear variable differential transformer (LVDT) records the penetration value in mm, while the load cell records the applied load. The test continues until the cone refuses to penetrate further even when additional load is applied.

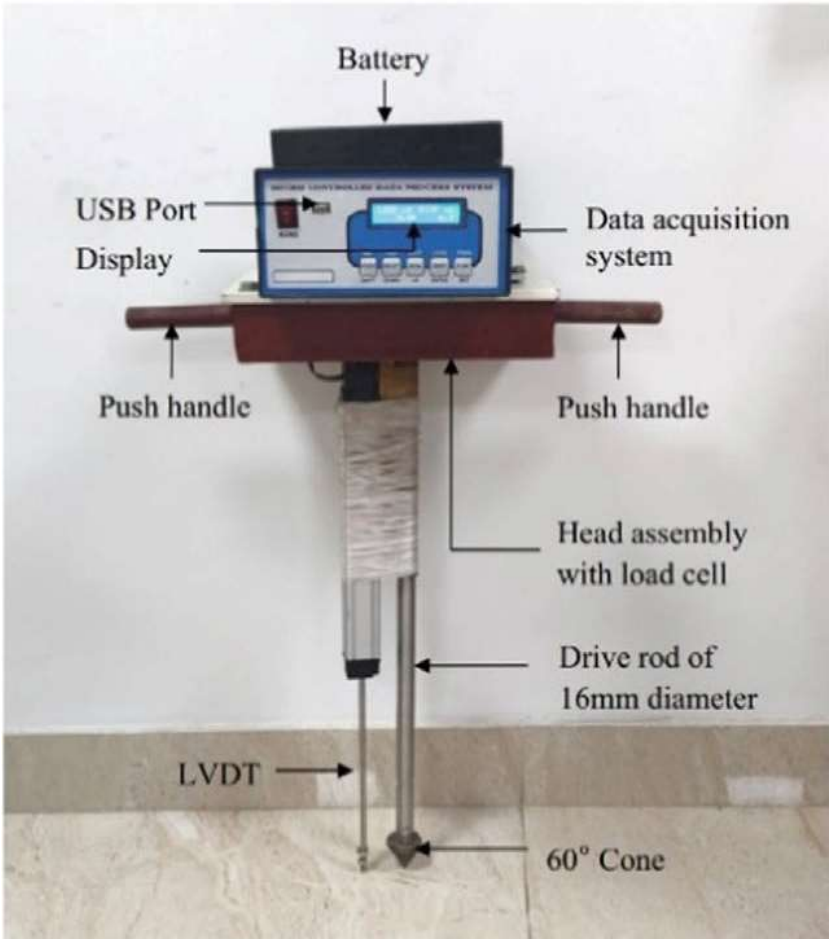

Fig. 3.9 Digital static cone penetrometer

In this test, a steel tank measuring 650 mm length, 450 mm breadth & 300 mm depth were used. Upper 150 mm of soil was treated as the soft subgrade soil layer and 150 mm bottom soil layer treated as natural soil. For cohesionless and unsaturated soils, dynamic loading from vehicles can result in problems such as liquefaction, mud pumping, or shear fluidization. Since the soil used in this study is cohesionless and unsaturated, it is prone to shear fluidization (Das and Luo, 2016). Previous research suggests that improving resistance to shear fluidization requires reinforcing the subgrade within 0.25–0.5H of the total soil depth (Boban et al., 2024). In present research work use a tank depth (H) is 300 mm, this test was 150 mm adopted as the soft subgrade soil thickness. The test locations inside the tank are illustrated in Figure 3.10. Several tests were conducted using different reinforcement layers. Geogrid and geotextile reinforced were placed at different depths like 50 mm, and 100 mm.

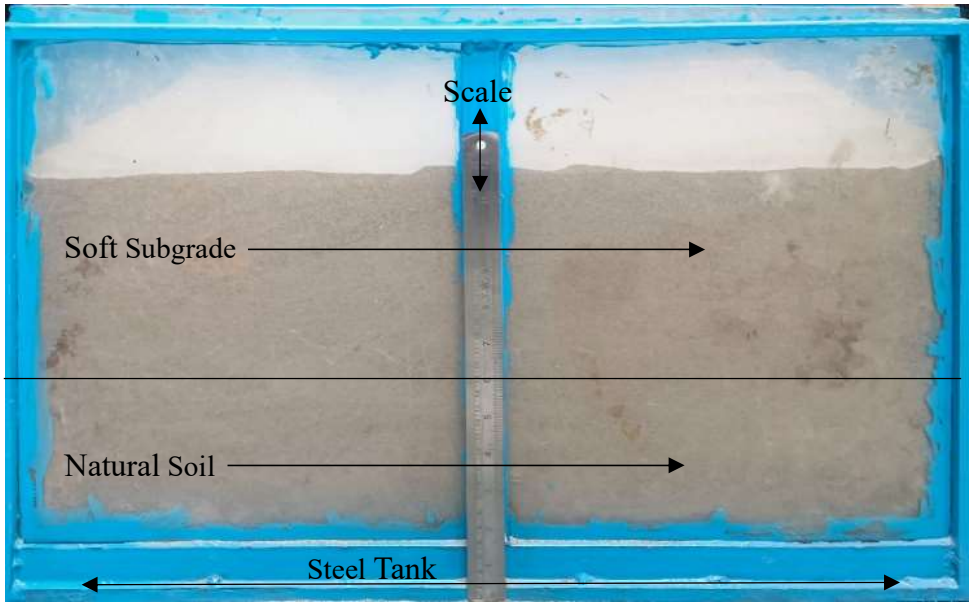

Fig. 3.10 Steel tank filled with sandy soil (ITS and Soil Dynamics laboratory, DTU, Delhi)

3.7 Dynamic Cone Penetrometer (DCP) Test

DCP used in this study illustrated in Figure 3.11, conforms to the requirements of ASTM D6951-03.

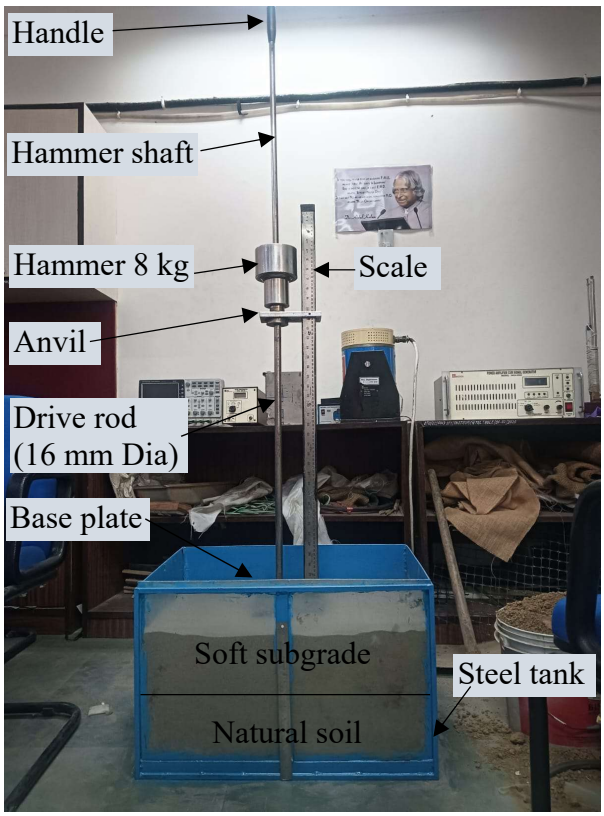

Fig. 3.11 Dynamic cone penetrometer (ITS and Soil Dynamics laboratory, DTU, Delhi)

A cone having 60-degree cone tip angle and a base Dia of 20 mm was attached to a rod measuring 16 mm in diameter. During the test, the rod was kept in a vertical position & 8 kg hammer was raised to a height of 575 mm before being released freely to penetrate compacted subgrade soil. While lifting the hammer, proper care should be ensured so that it reaches the lower stop of the handle without causing the cone to move upward before being released. Any improper handling during lifting or dropping can introduce errors in the DCP measurements. The penetration recorded from the first hammer blow is ignored, a smaller area is provided at the cone tip during initial impact compared to subsequent blows. The cone was designed with a slightly larger Dia than rod so that soil resistance could be mainly developed around the cone (George et al., 2009). For each hammer blow, the corresponding penetration depth is measured. DCPI was defined as penetration depth per no. of blows and expressed in mm per blow. It was calculated using Equation 3.6 (Chennarapu et al., 2018). As an alternative, DCPI was determined by plotting the penetration depth against total no. of blows and calculating slope of best-fit line (Ampadu and Fiadjoe, 2015).

$$DCPI = \frac{P_{(i+1)} - P_{(i)}}{N_{(i+1)} - N_{(i)}} \quad \ldots\ldots\ldots (3.6)$$

Where, DCPI represents the dynamic cone penetration index; $P_{(i)}$ and $P_{(i+1)}$ denote the cone penetration value corresponding to the (i) th & (i+1) th successive hammer strikes, respectively, measured in mm & N(i) and N(i+1) indicate the number of blows associated with P(i) and P(i+1), respectively.

DCP test results were evaluated to obtain representative DCPI values for the soil subgrade using the relationship given in Equation 3.7 (Chennarapu et al., 2018). The results obtained from DCP test were further utilized to distinguish the interfaces of the different soil layer. These boundaries determined from significant changes in slope of graph plotted between total blow count and penetration depth.

$$DCPI_{avg} = \frac{\sum_i^N DCPI}{N} \quad \ldots\ldots\ldots (3.7)$$

Where N denotes total no. of DCPI readings recorded within specified penetration depth.

3.8 Geosynthetic Material as a Reinforcement

This study used geosynthetic material like geogrid and geotextile. Geosynthetics are placed as reinforcement in different depths such as 50 mm and 100 mm. In this study geotextile shown in Figure 3.12 is a woven fabric made from polypropylene multifilament yarns. It is durable and

can resist chemicals and microorganisms commonly present in soil (Singh et al., 2020). Geotextile properties shown in Table 3.5 (Singh et al., 2020). In this study use biaxial geogrid material shown in Figure 3.13, was manufactured using a perforated polypropylene sheet with interconnected ribs, it helps control the sideways movement of granular soil by improving interface friction (Boban et al., 2024). Geogrid properties shown in Table 3.6 (Singh et al., 2020).

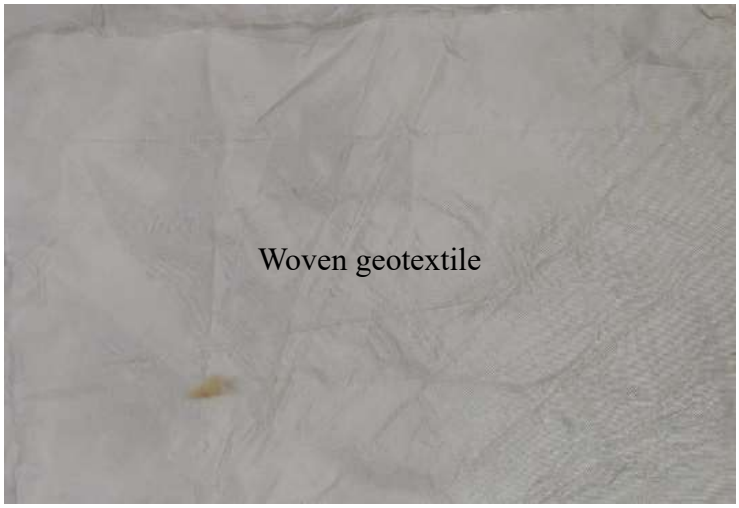

Fig. 3.12 Woven geotextile used in this study

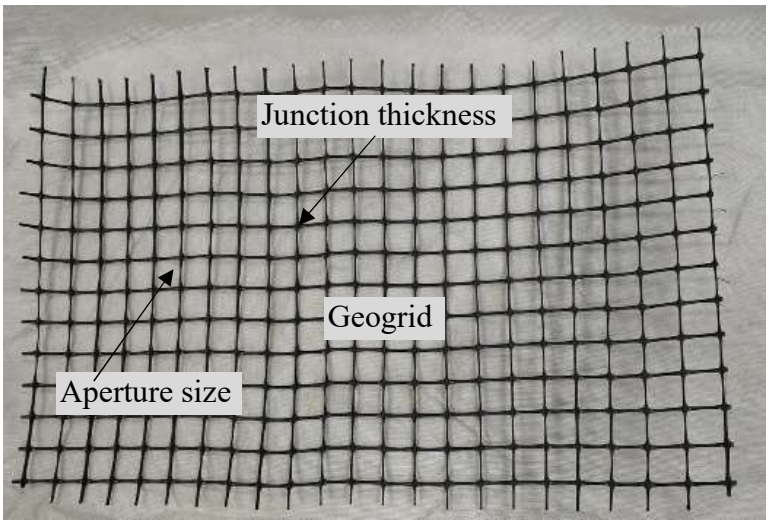

Fig. 3.13 Bi-axial geogrid

Table 3.5 Properties of geotextile (Singh et al., 2020)

Properties	Results/Values
Tensile strength (kN/m)	45 x 34 (MD x CMD)
Puncture strength (kN)	0.48
Apparent opening size (mm)	0.075
Fabric weight per unit surface area (g/m^2)	200

Table 3.6 Properties of geogrid (Singh et al., 2020)

Characteristics	Properties	Results/Values
Physical	Geogrid shape	Bi-axial geogrid
	Color	Black
	Shape of the openings	Four-cornered
	Polymer category	PP (Polypropylene)
Engineering Properties	Aperture dimension (mm)	30 x 30 (MD x CMD)
	Tensile rigidity at 0.5% strain (kN/m)	550 x 350 (MD x CMD)
	Width of transverse ribs (cm)	0.26
	Thickness of longitudinal ribs (cm)	0.38
	Thickness at junction (cm)	0.6
Performance	Friction interaction coefficient (soil/geosynthetics)	1.78 at 10 kN/m^2 and 1.14 at 20 kN/m^2
	Factor related to installation damage	1

3.9 CBR-DCPI Correlation

The DCP results can be correlated with California bearing ratio (CBR) values using empirical relationships. A commonly used correlation is following equation 3.8 (Singh et al., 2020).

$$CBR = \frac{292}{(DCPI)^{1.12}} \quad \text{..... (3.8)}$$

Also calculated improvement percentage formula is following equation 3.9.

$$\text{Improvement (\%)} = \frac{P_{Reinforced} - P_{Uneinforced}}{P_{Unreinforced}} \text{ x } 100 \quad \text{..... (3.9)}$$

Where, $P_{Unreinforced}$ = Penetration (unreinforced), $P_{Reinforced}$ = Penetration (reinforced)

CHAPTER 4

RESULT AND DISCUSSIONS

4.1 Assessment of Soil Resistance Using DSCPT

DSCPT was conducted on sandy soil at two locations 50 mm and 100 mm depth placed reinforcement from top layers of sandy soil. When the driving rod was placed close to the soil surface, the cone sank deeply on its own because the poorly graded soil offered very little resistance to its penetration shown in Figure 4.1 front view of steel tank with digital static cone penetration test.

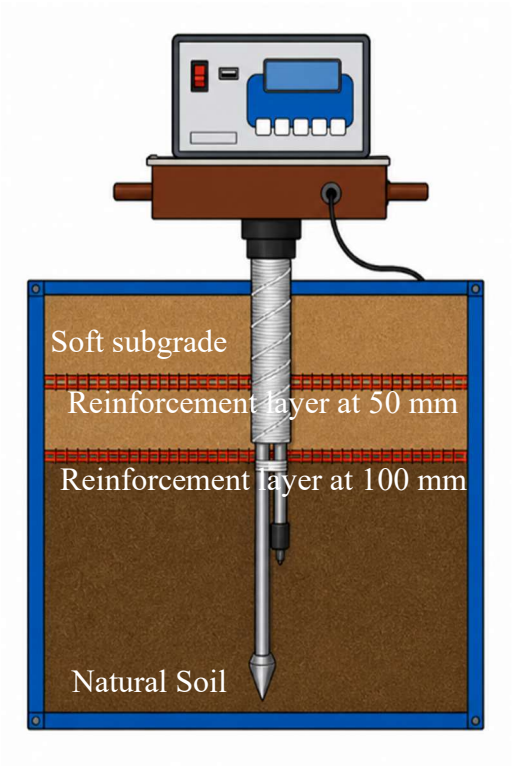

Fig. 4.1 Schematic representation DSCPT test setup front view

The DSCPT test was performed under two different conditions, which are listed below:

a. Without reinforcement
b. With reinforcement (like geogrid and geotextile reinforcement)

Without any reinforcement, the cone sinks into the soil subgrade under its own weight because the soil offers almost no resistance. After it reaches a certain depth, the soil becomes denser due to the overburden pressure, which helps it develop some strength. The graph clearly illustrates how reinforcement improves the behavior of soft subgrade soil under applied load. Without

reinforcement, the soil deforms quickly under minimal load because of its weak structure, leading to high displacement and lower bearing strength. With reinforcement, both the geogrid and geotextile restrict lateral movement of soil and distribute the applied load more efficiently.

4.1.1 Effect of Reinforcement (like Geogrid & Geotextile) at 50 mm Depth

The load-displacement graph compares three conditions: without reinforcement, with geogrid, and with geotextile at 50 mm depth shown in Figure 4.2.

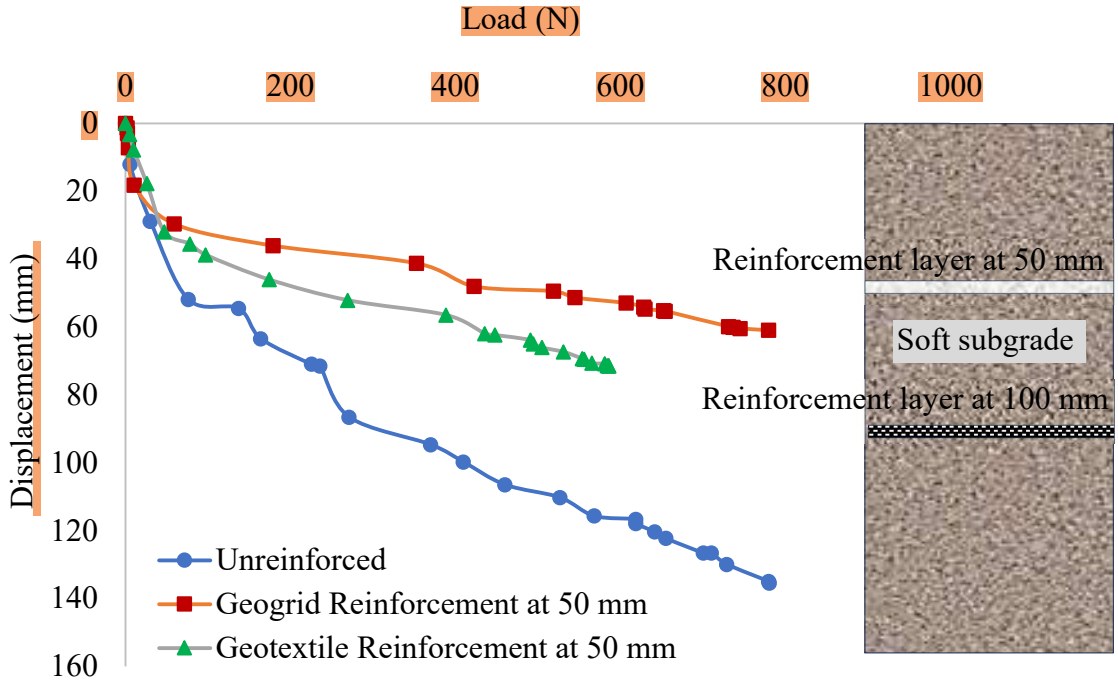

Fig. 4.2 Load displacement curve without and with reinforced at 50 mm depth

The results show that the unreinforced soil undergoes large displacement for relatively lower loads, reaching nearly 780 N load at a displacement of about 136 mm. When geotextile is used, the load-carrying capacity increases noticeably and the soil resists higher loads at smaller displacements, reaching around 580 N at nearly 71 mm displacement. Among the three, the geogrid-reinforced soil performs the best, showing the highest load resistance of nearly 780 N, but at a much smaller displacement of about 60 mm, indicating a significant improvement in stiffness and stability. The geogrid performs better than the geotextile. This is likely due to the geogrid's higher tensile rigidity and its efficiency to interlock properly with the confined soil, resulting in improved load transfer. The reduced displacement observed in both reinforced cases demonstrate increased soil stiffness, quicker load mobilization, and delayed failure. The

geogrid's steeper load–displacement curve indicates a stronger and more rigid response compared to geotextile. Observation data and collection listed in Table 4.1.

Table 4.1 Observation with & without reinforcement at 50 mm depth

	Without reinforcement		With Geogrid at 50mm		With Geotextile at 50mm	
S.I No.	Load (N)	Disp. (mm)	Load (N)	Disp. (mm)	Load (N)	Disp. (mm)
1	00	00	00	00	00	00
2	5.5	12	2	1.3	5	3.3
3	30	28.8	2.5	2.9	10	7.8
4	76	51.8	3.5	7.1	26	17.7
5	137	54.5	10.5	18.2	47	31.9
6	164	63.4	59	29.6	78	35.5
7	225.5	70.9	179	36	97	38.7
8	235.5	71.4	353	41.2	174.5	46
9	271	86.5	422.5	48	269.5	52.1
10	370	94.6	519	49.4	388.5	56.4
11	409.5	99.7	545	51.3	435.5	61.9
12	460	106.4	607	52.9	448	62.3
13	526.5	110.2	628.5	54.1	491	63.8
14	568	115.6	630	54.7	494.5	64.9
15	618.5	116.6	652.5	55.1	505	66
16	618.5	117.8	654.5	55.3	531	67.3
17	641.5	120.3	731	59.8	554	69.3
18	655	122.2	736.5	60	556	69.5
19	700.5	126.5	745	60.4	565.5	70.6
20	710	126.5	779.5	60.9	581	70.8
21	729	129.9	---	---	584	71.3
22	779.5	134.9	---	---	585.5	71.3
23	780.5	135.4	---	---	586	71.4

4.1.2 Effect of Reinforcement (like Geogrid & Geotextile) at 100 mm Depth

The load-displacement curve represented in Figure 4.3 show the behavior of subgrade under three conditions: without reinforcement, with geogrid, and with geotextile at 100 mm depth. The

unreinforced soil exhibits large displacement for increasing load, reaching about 780 N at nearly 136 mm displacement. When geotextile is placed at 100 mm depth, the load-bearing capacity improves; the soil carries around 730 N load at approximately 112 mm displacement, showing better stiffness than the unreinforced case. The geogrid-reinforced condition performs the best among the three, reaching nearly 700 N load at a smaller displacement of about 102 mm, indicating the highest improvement in load resistance and reduced deformation.

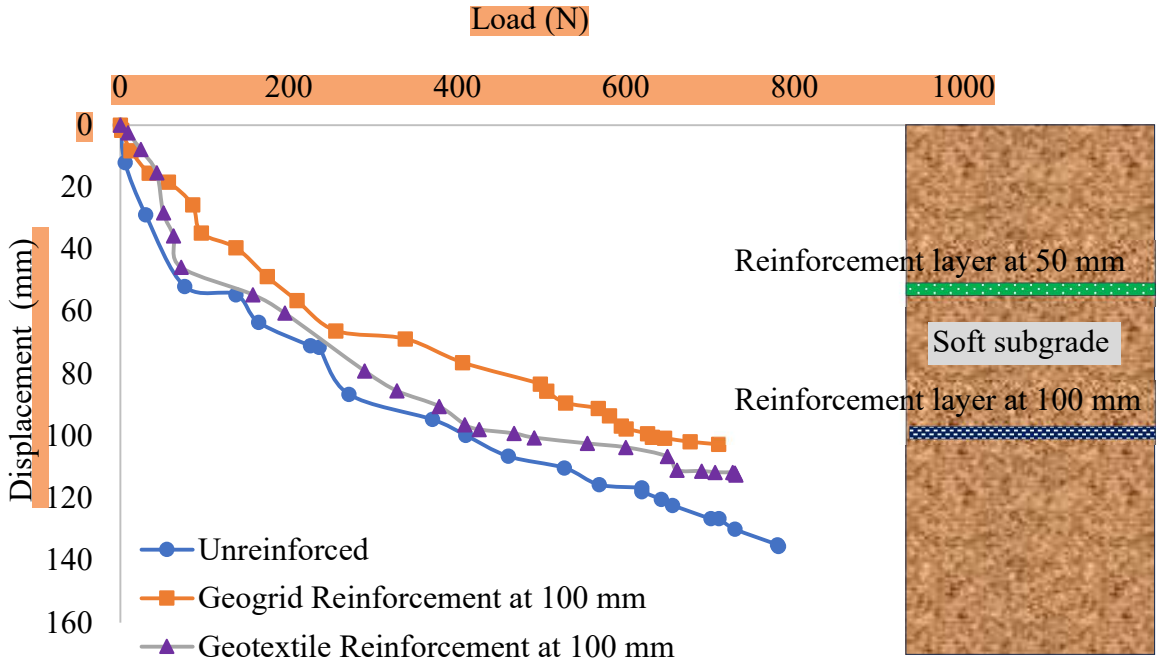

Fig. 4.3 Load displacement curve without and with reinforced at 100 mm depth

The graph clearly shows that reinforcing the soil at 100 mm depth enhances its load-carrying ability and reduces overall displacement. Without reinforcement, the soil continues to deform gradually as the load increases, reflecting its weak structural support. Both geogrid and geotextile reinforcement provide confinement and help distribute the applied load, which results in quicker mobilization of strength and a steeper load–displacement response. Between the two reinforcement materials, geogrid performs slightly better than geotextile at this depth. This may be due to its higher tensile strength and better interlocking characteristics, which improve soil–reinforcement interaction. Although the improvement at 100 mm depth is noticeable, the reinforcement's effectiveness is slightly reduced compared to shallower reinforcement, which is expected because reinforcement placed deeper tends to engage later during loading. Observation data and collection shown in Table 4.2 and also shown in Table 4.3 for improvement percent comparison between reinforced and unreinforced soil conditions of static cone penetration test.

Table 4.2 Observation and data collection with and without reinforcement at 100 mm depth

	Unreinforced		Geogrid reinforced at 100mm		Geotextile reinforced at 100mm	
S.I No.	Load (N)	Disp. (mm)	Load (N)	Disp. (mm)	Load (N)	Disp. (mm)
1	00	00	00	00	00	00
2	5.5	12	1.5	1.6	9	2.4
3	30	28.8	12.5	8.2	24	7.8
4	76	51.8	34	15.4	43	15.3
5	137	54.5	57	18.3	51	28.2
6	164	63.4	85.5	25.6	63	35.6
7	225.5	70.9	96	34.7	72	45.7
8	235.5	71.4	137	39.4	157	54.5
9	271	86.5	174	48.7	195	60.4
10	370	94.6	209.5	56.4	289.5	79
11	409.5	99.7	255.5	66.1	328	85.4
12	460	106.4	338	68.7	378	90.4
13	526.5	110.2	406	76.3	408.5	96.3
14	568	115.6	498	83.2	425.5	97.8
15	618.5	116.6	505.5	85.5	467	99.1
16	618.5	117.8	528	89.3	491	100.5
17	641.5	120.3	567	91.05	554	102.3
18	655	122.2	580	93.45	599.5	103.6
19	700.5	126.5	594	96.7	649	106.5
20	710	126.5	600	97.6	660.1	110.9
21	729	129.9	625.5	99.2	689.5	111.2
22	779.5	134.9	631	100.3	705.5	111.6
23	780.5	135.4	645.5	100.6	726.5	111.6
24	---	---	676	101.8	729	111.8
25	---	---	709.5	102.6	730.1	112.5

Table 4.3 Comparison between reinforced soil of SCPT improvement percent

Reinforced at 50 mm		Reinforced at 100 mm	
Improvement (%)		Improvement (%)	
Geotextile	Geogrid	Geotextile	Geogrid
144 %	225 %	41.09 %	61.36 %

4.2 Evaluation of Subgrade Strength by DCP

This study DCP was performed on sandy soil, and the schematic arrangement is presented in Figure 4.4. The test was performed to evaluate strength behavior of subgrade soil at various condition with reinforcement. A direct correlation between the no. of hammer blows & corresponding penetration depth were obtained from the test, which aided in evaluating the soil resistance and stiffness characteristics. In this study, the performance of soil was evaluated under two different conditions:

a. Without reinforcement
b. With reinforcement (geosynthetic material like geogrid and geotextile)

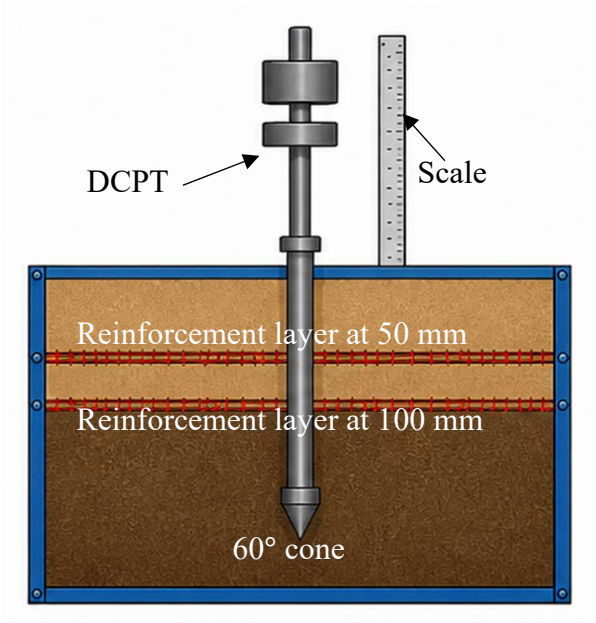

Fig. 4.4 Schematic diagram of laboratory test tank showing reinforced soft subgrade and DCP test setup

The reinforcements were placed at two different depths, namely 50 mm and 100 mm, to understand the influence of reinforcement position on subgrade behavior. The unreinforced soil

exhibited the highest penetration depth, the penetration increased rapidly during the initial stages of loading, indicating that the soil offered relatively low resistance to the applied impact energy.

4.2.1 Effect of Reinforcement Type on Soil Penetration Characteristics at 50 mm Depth

The result of DCP test was presented in form of penetration depth versus no. of blows & the recorded observations were summarized in Table 4.4. The graph presented in Figure 4.5 clearly indicates that the penetration depth showed an increase with in the number of blows under all testing conditions.

Table 4.4 Observation and calculation of DCPI values with penetration depth for reinforced and unreinforced soil at 50 mm

Unreinforced soil			Reinforced soil (Geogrid) at 50 mm		Reinforced soil (Geotextile) at 50 mm	
No. of blows	Penetration depth (mm)	DCPI (mm/blow)	Penetration depth (mm)	DCPI (mm/blow)	Penetration depth (mm)	DCPI (mm/blow)
0	0	--	0	--	0	--
1	55	50	30	15	28	20
2	105	15	45	10	48	10
3	120	15	55	15	58	10
4	135	10	70	12	68	12
5	145	15	82	10	80	08
6	160	05	92	08	88	07
7	165	05	100	05	95	05
8	170	03	105	03	100	02
9	173	--	108	--	102	--
DCPI (avg.) = 14.75			DCPI (avg.) = 9.75		DCPI (avg.) = 9.25	

The unreinforced soil exhibits the highest penetration values throughout the test. At higher blow counts 9 blows, the penetration reaches 173 mm, indicating low resistance and weak subgrade strength. soils reinforced with geogrid and geotextile at 50 mm depth show a noticeable reduction in penetration. For similar blow counts, the penetration depth reaches 108 mm and 102 mm respectively.

A geogrid reinforcement performs slightly better than geotextile, as it consistently shows lower penetration values at each stage of loading.

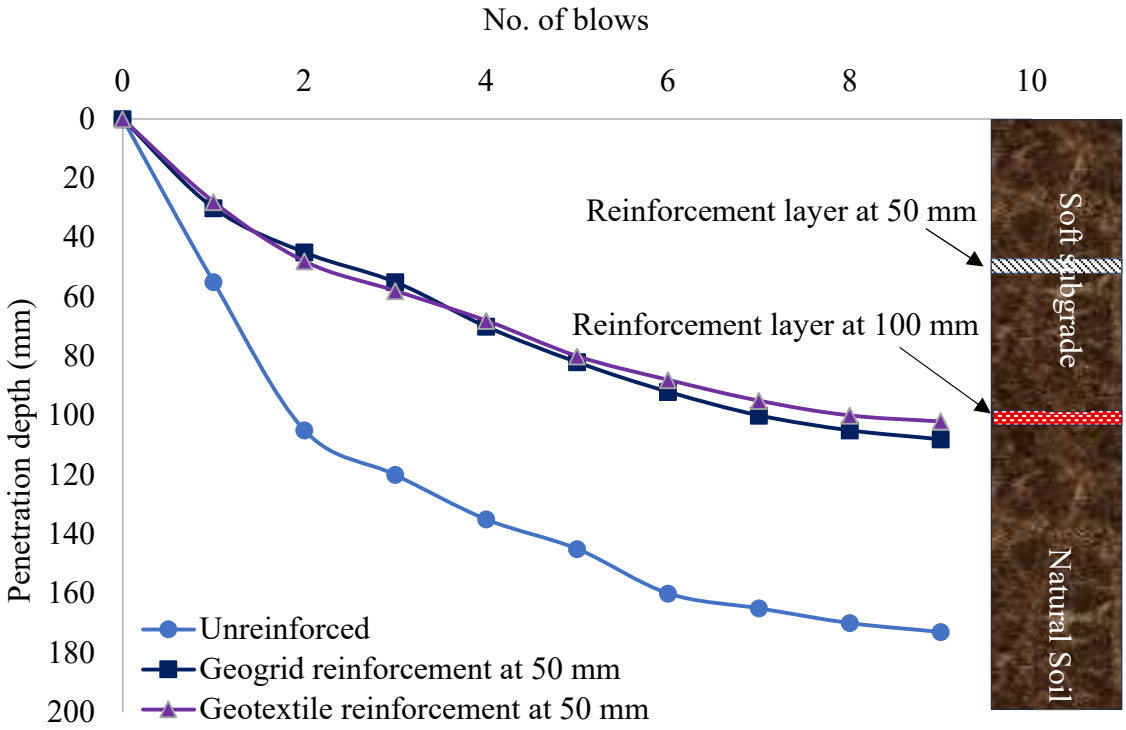

Fig. 4.5 Penetration depth v/s no. of blows for reinforced and unreinforced soil at 50 mm

The reduction in penetration depth in reinforced samples indicates an increase in soil stiffness and resistance. The unreinforced soil allows easy penetration due to the absence of side restraint and structural stability. The performance improvement achieved by geogrid reinforcement was mainly attributed to its interlocking action with the soil particles. The interlocking mechanism was responsible for restricting particle movement and distributing the applied load over a larger area, thereby reducing penetration. Geotextile reinforcement acts more like a separation and tension membrane layer. While it improves the behavior of the soil, its contribution to load distribution is comparatively less than that of geogrid. This explains the slightly higher penetration values observed in the geotextile case. A more significant difference between reinforced and unreinforced soil was observed an increase with in the no. of blows. This suggests that reinforcement is particularly effective under repeated or cyclic loading conditions, such as traffic loads in pavements.

4.2.2 Effect of Reinforcement Type on Soil Penetration Characteristics at 100 mm Depth

The DCP test results presented in the graph shown in Figure 4. penetration depth v/s no. of blows for three conditions unreinforced soil, geogrid reinforcement at 100 mm depth, and geotextile reinforcement at 100 mm depth.

Table 4.5 Observation and calculation of DCPI values with penetration depth for reinforced and unreinforced soil at 100 mm

Unreinforced soil			Reinforced soil (Geogrid) at 100 mm		Reinforced soil (Geotextile) at 100 mm	
No. of blows	Penetration depth (mm)	DCPI (mm/blow)	Penetration depth (mm)	DCPI (mm/blow)	Penetration depth (mm)	DCPI (mm/blow)
0	0	--	0	--	0	--
1	55	50	32	20	35	25
2	105	15	52	18	60	15
3	120	15	70	15	75	12
4	135	10	85	13	87	14
5	145	15	98	07	101	10
6	160	05	105	10	111	07
7	165	05	115	10	118	03
8	170	03	125	05	121	03
9	173	--	130	--	124	--
DCPI (avg.) = 14.75			DCPI (avg.) = 12.25		DCPI (avg.) = 11.13	

The curve patterns clearly indicated an improvement in strength of the subgrade due to the addition of reinforcement materials. For the unreinforced soil penetration depth increases rapidly with no. of blows. Even at a comparatively small number of blows, penetration is significantly higher, indicating lower resistance and weak strength of soil. This trend reflects typical behavior of poorly graded sand, where particle interlocking is limited and resistance to penetration is relatively low. A noticeable reduction in penetration depth was observed in both geogrid and geotextile-reinforced soils for the same no. of blows. This suggested that the reinforcement improved stiffness and load-bearing capacity of soil. The observed improvement was mainly attributed to the confinement effect developed by the reinforcement layers, which restrict lateral

movement of soil particles and increase interlocking. Between the two reinforcement types, the geogrid-reinforced soil generally shows slightly better performance compared to the geotextile, especially at higher numbers of blows. Another important observation is that the rate of increase in penetration depth reduces significantly in reinforced cases as compared to unreinforced soil. These finding support effectiveness of geosynthetic material in reducing deformation & increasing the service life of flexible pavements. observation and collection data shown in Table 4.5 and also shown in Table 4.6 for improvement percent comparison between reinforced and unreinforced soil conditions of dynamic cone penetration test.

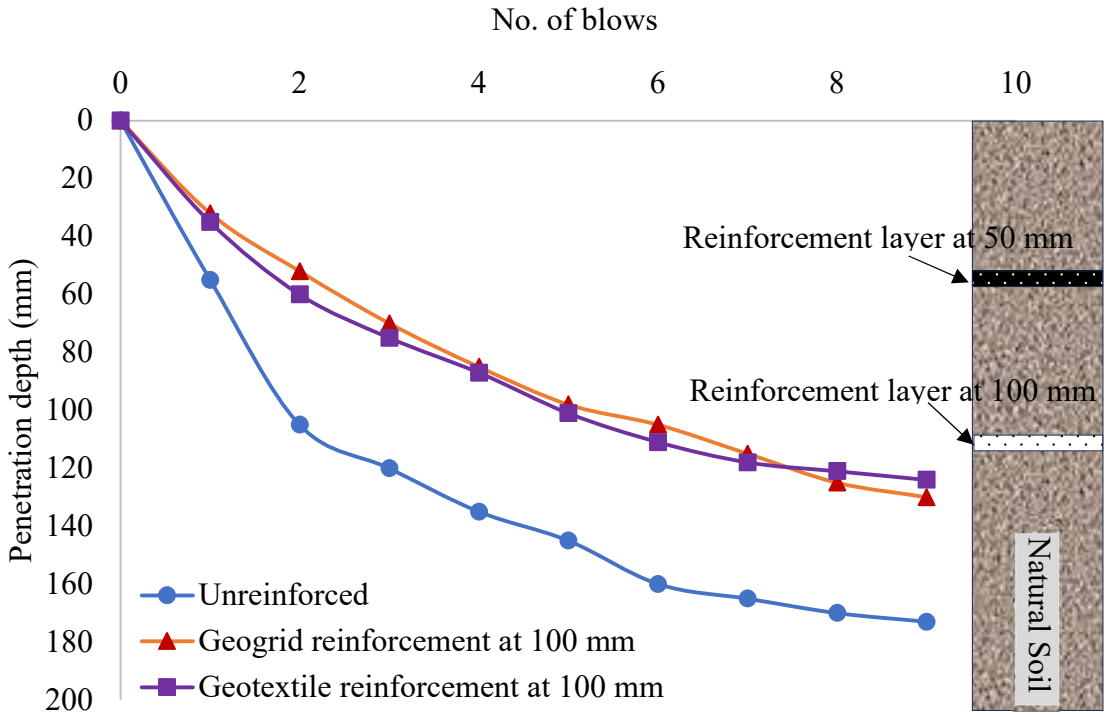

Fig. 4.6 Penetration depth v/s no. of blows for reinforced and unreinforced soil at 100 mm

Table 4.6 Comparison between reinforced soil of DCPT improvement percent

Reinforcement at 50 mm		Reinforcement at 100 mm	
Improvement (%)		Improvement (%)	
Geotextile	Geogrid	Geotextile	Geogrid
200 %	300 %	166.67 %	200 %

4.3 CBR Result

CBR and DCPI calculation data from equation 3.6, 3.7 and 3.8 presented in Table 4.7 calculated DCPI & CBR value.

Table 4.7 Calculated DCPI and CBR values

Unreinforced soil		Reinforced soil (Geogrid) at 50 mm		Reinforced soil (Geogrid) at 100 mm		Reinforced soil (Geotextile) at 50 mm		Reinforced soil (Geotextile) at 100 mm	
DCPI	CBR (%)	DCPI	CBR (%)	DCPI	CBR (%)	DCPI	CBR (%)	DCPI	CBR (%)
14.75	14.33	9.75	22.79	12.25	17.65	9.25	24.17	11.13	19.65

Unreinforced soil shows a higher DCPI (mm/blow), which corresponds to lower CBR values, indicating weak subgrade. Geogrid reinforced soil has the lowest DCPI, resulting in higher CBR values, indicating improved strength. Geotextile reinforced soil also shows improved CBR compared to unreinforced soil but slightly lower than geogrid. Maximum improvement in CBR was observed for reinforcement at 50 mm depth. DCP-based CBR estimation provides a reliable and practical approach for subgrade evaluation.

37

CHAPTER 5

CONCLUSION AND FUTURE SCOPE

5.1 Conclusion

Performance of geogrid and geotextile reinforcement in weak subgrade soil was investigated in present study using SCPT & DCPT. The behavior of reinforced soil was evaluated in comparison with unreinforced soil by placing reinforcement layers at depths of 50 mm and 100 mm. Based on the experimental results and detailed analysis, the following conclusion was written:

1. A significant improvement in load carrying capacity and penetration resistance of soil was observed after the addition of geosynthetic reinforcement compared to the unreinforced condition. Improved performance of the reinforced soil was clearly observed from both SCPT and DCPT results. In SCPT results unreinforced soil shown higher displacement under lower loads indicating lower stiffness and bearing resistance. Reinforced specimens showed reduced settlement and higher resistance against penetration.

2. In the SCPT results all reinforcement conditions, the improvement in cone resistance was about 225% compared to unreinforced soil, while geotextile reinforcement at 50 mm showed an improvement of cone resistance about 144%. For reinforcement at 100 mm depth, geogrid showed an improvement of cone resistance about 61.36%, whereas geotextile showed an improvement of cone resistance about 41.09%. Reinforcement placed at 50 mm depth performed better than reinforcement placed at 100 mm depth. This indicates that reinforcement closer to the loading surface provides greater confinement and distributes stresses more effectively.

3. In the DCPT results also confirmed the strengthening effect of reinforcement. The average DCPI value decreased from 14.75 mm/blow for unreinforced soil to 9.75 mm/blow for geogrid reinforcement and 9.25 mm/blow for geotextile reinforcement at 50 mm. Reinforcement at 100 mm depth showed comparatively higher DCPI values than reinforcement at 50 mm depth, confirming that shallow placement of reinforcement is more effective for improving subgrade behavior. Lower DCPI values indicate higher penetration resistance and improved soil strength. The improvement obtained from DCPT analysis showed that geogrid reinforcement at 50 mm depth produced nearly 300% improvement, while geotextile at 50 mm showed about 200% improvement. At

100 mm depth, geogrid reinforced and geotextile reinforced showed improvements of about 200% and 166.67%, respectively.

4. CBR values estimated from DCPI correlations also increased considerably due to reinforcement. A CBR value of 14.33% was recorded for the unreinforced soil, whereas the addition of geogrid reinforcement at a depth of 50 mm increased the CBR value to 22.79%, and geotextile reinforcement at the same depth improved it to 24.17%. This confirmed that geosynthetic reinforcement improved of weak subgrade.

5. Comparison between SCPT and DCPT results showed an almost similar trend in behavior. Better performance was observed in reinforced soil compared to unreinforced soil in both tests, while the maximum improvement was achieved with geogrid reinforcement placed at a shallow depth. The consistency between the two testing methods validates the reliability of the experimental results.

6. Overall, the study demonstrated that geosynthetic reinforcement an effective technique for improving strength & stability of weak subgrade soil. Reinforcement placed near the surface, particularly geogrid at 50 mm depth, was found to be the most efficient configuration for reducing penetration and improving load carrying capacity.

5.2 Future scope

- The experimental findings of this study may be validated through full-scale field trials under actual traffic loading conditions to evaluate real-time behavior of reinforced unpaved road.
- Long-term behavior of reinforced subgrades may be examined by considering repeated loading.
- The combined application of different types of geosynthetics, including natural and synthetic reinforcements, may be explored to improve sustainability and cost-effectiveness.
- Advanced numerical modeling and finite element analysis may be carried out to simulate stress distribution, deformation behavior, and reinforcement mechanisms in reinforced subgrade systems.
- Using large-scale field tests under wheel loads.
- Studying multilayer geosynthetic material or composite material.
- Evaluating long-term performance under repeated loading.

APPENDIX – I

Acceptance Letter 1st Conference

Dear Nitish Kumar,

Congratulations! We are pleased to inform you that your paper, **"Effect of Geosynthetic Reinforcement in Unpaved Road Using Static Cone Penetration Test"** , has been **accepted** for Oral/Poster presentation at **5th International conference on Advances in Science,Engineering &Technology (ICASET)** accredited by **Continuous Professional Development (CPD)** in **India** on **2026-03-22 - 2026-03-23**.
This is a significant milestone in your research journey, and we are excited to have you join us!

Your submission has successfully passed our rigorous double-blind peer review and plagiarism check, demonstrating the significance and quality of your work.

Indexing & Publication:

Your paper will be submitted for evaluation and indexing in **Web of Science (BkCI)** and **SCOPUS** (terms and conditions apply). This will significantly boost the visibility and impact of your research. Alternatively, you can opt to publish your paper in a **Scopus-indexed journal**.

Session and SDG Alignment

Your paper will be presented in the **Powering Progress: Sustainable Industries & Innovation** session, which is focused on geotechnical reinforcement techniques, infrastructure durability enhancement, and cost-effective sustainable road engineering solutions that improve transportation resilience and support long-term industrial and economic development. This session directly aligns with the **SDG 7, 8, 9, and 12** (Sustainable Development Goal) and will contribute to discussions surrounding renewable energy efficiency, sustainable industrial automation, green job creation, and resource-efficient technological solutions for long-term environmental sustainability. Your research plays a crucial role in advancing solutions to these global challenges.

CPD Benefits

As an accepted presenter, you will receive a **CPD Certificate** for your participation and be eligible for **CPD points**. You will also enjoy **1-year free iCPD membership**, offering you access to exclusive resources and further professional development opportunities.

Next Steps:

To complete your participation, kindly **register** for the conference by **2026-03-09**.

Registration Link : Click Here

Use the coupon code **EB250** for a 250 INR discount on your registration.

Best regards,
Mohammed Ibrahim M
+91 63690 25172

Payment Receipt 1st Conference

Technoarete Group
Integrating Researchers to Incubate Innovation

RECEIPT

M/s. Technoarete Research & Development Association. Rais Towers, 2054/B, 2nd Floor, West block, 2nd Ave, Anna Nagar, Chennai, Tamil Nadu 600040 Contact: +91 9944046574 **GSTN: 33AAFCT7109P2ZX** **CIN : U80221TN2016NPL104388**	**DATE:** 2026-02-28 03:31:32 **Payment MODE:** Online Payment **Order I'D** 69a260bd121d4
BILL TO: NITISH KUMAR Shahbad Daulatpur, Main Bawana Road, Rohini Sector 17, 110042	

Sr.No	DESCRIPTION	Amount	
1	ICASET_ 2026	4720	
		Internet Handling Charges (2.5%)	118
		Total	4588.00

Amount in Words: Four Thousand Five Hundred and Eighty Eight Rupees

This is System Generated Receipt so, signature not required

THANK YOU FOR YOUR REGISTRATION!

APPENDIX – II

Acceptance Letter 2nd Conference

INRI

Acceptance Letter

Date: ICGECE-26

Conference Name : **International Conference on Geotechnical Engineering and Civil Engineering Solutions (ICGECE-26)**

Conference Venue : **Lucknow - India**

Authors Name : **Nitish Kumar, Kshitij Gaur, Ashutosh Trivedi**

Paper Title : **Improvement of Soft Subgrade Using Geosynthetics: A Dynamic Cone Penetration Test Investigation**

Paper ID : **INRI_60345**

Dear Authors,

We are pleased to inform you that your paper has been accepted by the review committee for Oral Presentation at the **International Conference on Geotechnical Engineering and Civil Engineering Solutions (ICGECE-26) which will be held in 24th May 2026 Lucknow - India**

Your paper will be published in the conference proceeding and well reputed journal after registration.

Please register as soon as possible in order to secure your participation:

Conference Link: https://inrinetwork.org/conf/fee-details.php?id=101018203

You are requested to release the payment and mail us the screen of successful payment release with your name and title of paper to confirm your registration.

Sincerely,

International Network for Research & Innovation INRI

Organizing Committee Head
International Network for Research & Innovation (INRI)

+91-96770 07228
info@inrinetwork.org
www.inrinetwork.org

Payment Receipt 2nd Conference

Online Payment Receipt

INRI

International Conference on Geotechnical Engineering and Civil Engineering Solutions (ICGECE-26)

24th May 2026 | Lucknow - India

Reference ID	114505858554
Received on	13th May 2026
Amount Paid	5650 .INR

Name	Nitish Kumar
Email	ernitishce@gmail.com
Address	Delhi Technological University, India

Invoice / Items	Unit Price	Quantity	Amount
Registration for Online Presentation with Publication Paper ID: INRI_60345 Paper Title:Improvement of Soft Subgrade Using Geosynthetics: A Dynamic Cone Penetration Test Investigation	5650.INR	1	5650.INR
		Sub Total	5650.INR
		Net Amount	5650.INR

**This is computer generated online receipt, no signature required*

International Network for Research & Innovation INRI

www.inrinetwork.org

List Of Conferences / Publications and their proofs

17
10

1. Kumar, N., Gaur, K., and Trivedi, A. (2026). Effect of geosynthetic reinforcement in unpaved road using static cone penetration test. In *5th International Conferences on Advances in Science, Engineering & Technology (ICASET).*
2. Kumar, N., Gaur, K., and Trivedi, A. (2026). Improvement of soft subgrade using geosynthetics: A dynamic cone penetration test investigation. In *International Conferences on Geotechnical Engineering and Civil Engineering Solutions (ICGECE).*
3. Roy, P., Kumar, N., Gaur, K., and Trivedi, A. (2026). Effect of geogrid and bamboo-grid reinforcement in soil subgrade using dynamic cone penetration test. In *International Conferences on Geotechnical Engineering and Civil Engineering Solutions (ICGECE).*

Conference Certificate

Fig. 1 Conference certificate 1

Fig. 2 Conference certificate 2

Fig. 3 Conference certificate 3

PLAGIARISM REPORT

turnitin Page 56 of 56 - Integrity Submission Submission ID trn:oid:::27535:140490587